Theoretical study of thermodynamic and magnetic properties of transition metal carbide and nitride MAX phases

Ali Muhammad Malik, Jochen Rohrer,* and Karsten Albe†
Materials Modelling, Institute of Materials Science, Technical University of Darmstadt, 64287 Darmstadt, Germany

(Received 28 December 2022; revised 19 March 2023; accepted 28 March 2023; published 17 April 2023)

We systematically perform density-functional theory (DFT) calculations for all possible $M_{n+1}AX_n$ (MAX) phases with transition metal M=Sc to Au (excluding Tc), A in group IIIA-IVA, X=C, N, and $n = 1, 2, 3$, a total of about 1200 systems. The thermodynamic stability is determined by comparing the formation enthalpy (at 0 K) against all possible combinations of unary, binary, and ternary boundary phases (available from online DFT databases). Thereby, we identify 124 so far unknown phases (in terms of both experimental synthesis and other theoretical predictions), of which 54 are carbides and 70 are nitrides. Among all stable MAX phases, we identify nine with magnetic properties. In addition to already known and synthesized magnetic phases (Cr_2AlC, Cr_2GeC, Cr_2GaN, and Mn_2GaC), we predict five more MAX phases with magnetic ordering [Mn_2A(=Ge, Sn)C, Cr_3A(=Ga, Ge)N_2, and Cr_4A(=Ge)N_3]. Evaluating previously suggested descriptors for the stability of MAX phases [valence electron concentrations (VECs), differences in atomic radius difference ΔR_{at}, and differences in electronegativities $\Delta\chi$], we find that ΔR_{at} does not correlate with stability and stable phases are characterized by VEC < 5.5, $\Delta\chi > 1.5$. The reverse is, however, not true; for example, a MAX phase with VEC < 5.5 and $\Delta\chi > 1.5$ is not necessarily stable.

DOI: 10.1103/PhysRevMaterials.7.044408

I. INTRODUCTION

Layered ternary transition metal carbides and nitrides, combining properties of metals and ceramics, are known as MAX phases [1]. They are denoted by the general formula $M_{n+1}AX_n$, where M is a transition metal, A belongs to group III-IVA elements, X can be carbon and/or nitrogen, and n varies from 1 to 3 and represents the number of M_6X octahedra layers in the crystal structure (Fig. 1). Owing to their high stiffness, strength, and resistance to oxidation, some of MAX phases are used as structural materials in high-temperature oxidative environments [2–4]. They are also considered promising materials for electrical and thermal contacts due to their high electrical and thermal conductivities [5,6]. Over the past few years, the interest in MAX phases has resurfaced as a result of the discovery of MXenes—two-dimensional transition metal carbides, nitrides, and carbonitrides—upon chemical etching of A layers from a MAX precursor [7–9]. The significance of MAX phases as starting materials for MXene synthesis has caused vigorous efforts to expand the MAX family, both theoretically and experimentally [10–19]. In principle, this is possible because MAX phases offer a broad chemical space which can be exploited to incorporate "novel" transition metals or A elements into the structure and to fine-tune the properties (magnetism, exfoliability, etc.).

High-throughput computational approaches coupled with thermodynamic analysis can significantly accelerate the search for material design and provide guidance for experiments. This approach has been employed for finding new MAX phases. One of the early works was done by Dahlqvist *et al.*, who calculated formation enthalpies relative to all possible competing phases to predict the stabilities of certain MAX phases (A=Al, X=C and N, and M=Sc, V, Ti, etc.) [10]. Recently, another study using high-throughput density-functional theory (DFT) reported on the stabilities of nontraditional MAX compositions with nonconventional elements at the A site, e.g., Cu, Au, Cd, etc. [20]. Using the total DFT energies of the competing phases from the Open Quantum Materials Database (OQMD) [21,22], they calculated formation enthalpies which are positive in magnitude for M_2AlC (M=Ti, Cr, V) even though they have been synthesized. Consequently, the criterion for the stability limit was set to be +120 meV/atom, which can lead to overpredicting the stability limits. Few other works focused on evaluating the stabilities of double MM′AX phases as solid solutions or M-site ordered structures [19,23–26]. These studies employed thermodynamic treatments and made use of online DFT databases, e.g., OQMD [21,22], that can easily be integrated into the high-throughput workflow. In the majority of these reports, a major focus is put on carbides compared to nitrides (this also holds for experimental work). Therefore, the number of predicted and synthesized nitrides is less than that of carbides [27]. To date, a study that thoroughly investigates all possible transition metal MAX phases including carbides and nitrides with various n in its entirety and provides reliable guidelines for choosing compositions for experimental synthesis is still lacking. Moreover, online DFT databases are also rapidly expanding with new hypothetical phases. Therefore, it is important to evaluate the stability of MAX phases with

*rohrer@mm.tu-darmstadt.de
†albe@mm.tu-darmstadt.de

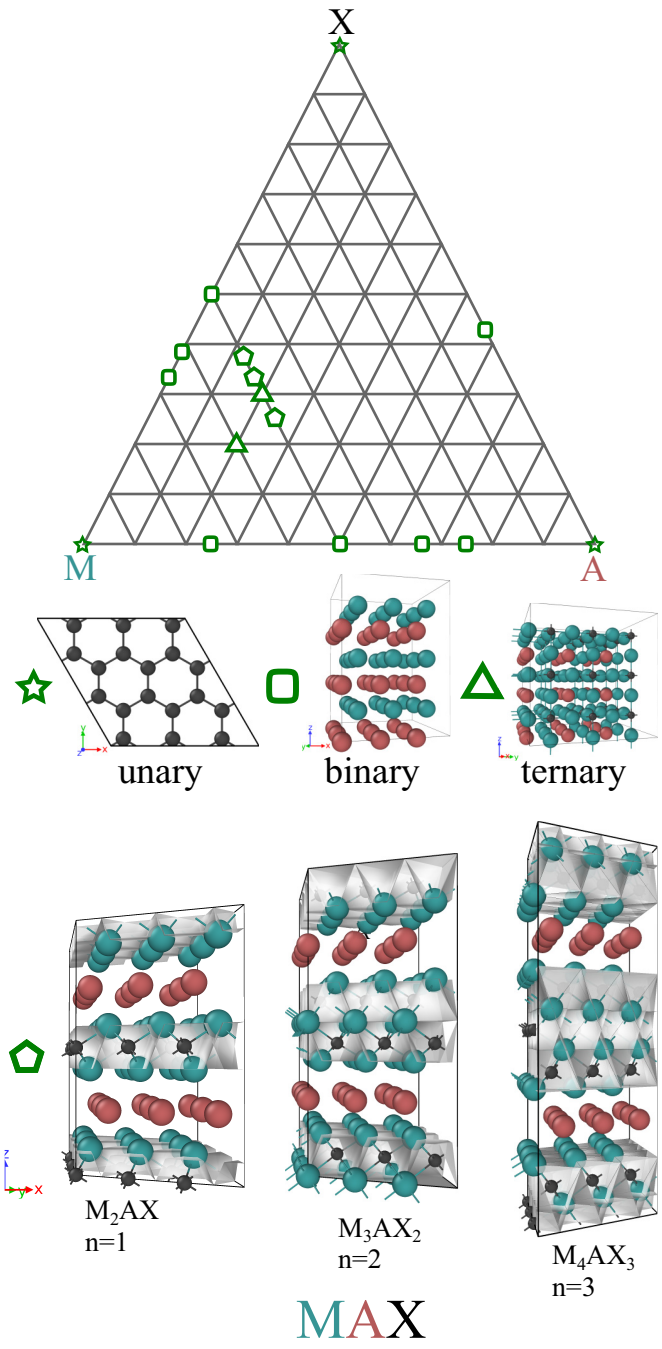

FIG. 1. Thermodynamic (meta)stability of individual MAX phases is inferred by the sign and magnitude of the calculated maximum formation enthalpies, relative to all possible combinations of known competing phases, including unaries, binaries, and ternaries, that are present in the M-A-X phase diagram [top panel; see Eq. (1)]. Boundary phases are retrieved from MP [28] and OQMD [21,22]. The bottom panel contains crystal structures of $(3 \times 3 \times 1)$ supercells of $n = 1, 2$, and 3 MAX phases along with other exemplary unary, binary, and ternary phases.

an updated set of competing phases. In this study, we intend to address this problem by evaluating the thermodynamics of MAX phases on the basis of the latest collection of competing phases that are available in DFT databases, i.e., the Materials Project (MP) [28] and OQMD [21,22]. To reliably determine stability, the uncertainty introduced by using the online database is minimized. Our predictions have excellent agreement with experiments, showing the accuracy of the overall methodology. Using the approach, we screen for (meta)stable MAX phases composed of M transition metals from Sc to Au, A in group IIIA-IVA, and X=C and N. This is accomplished by evaluating the formation enthalpies of MAX phases relative to all potential competing (boundary) phases accessible via OQMD [21,22] and MP [28]. On the basis of comparison with the experiment, a threshold value of formation enthalpy for (meta)stability is obtained. Using this, we predict 214 (meta)stable MAX phases, of which 90 have been synthesized or predicted by others so far. Furthermore, valence electron concentration (VEC) analysis suggests that all stable MAX phases are characterized by VEC below 5.5; the reverse, however, is not true.

II. METHOD

A. Thermodynamic approach

We characterize the stability of a MAX phase in terms of its maximum (absolute) formation enthalpy $\Delta_r H$ relative to all (unary, binary, and ternary) competing phases (CPs; see top panel of Fig. 1) that are accessible via the materials databases of MP [28] and OQMD [21,22]. Given the total DFT energy ϵ_{MAX} of a MAX phase, the maximum formation enthalpy is defined as

$$\Delta_r H = \max \left\{ \frac{\left| \epsilon_{\mathrm{MAX}} - \sum_{\mathrm{r} \in \mathrm{CP}} c_r \epsilon_r \right|}{N_{\mathrm{atoms}}} \right\} \text{all possible combinations of CPs}, \quad (1)$$

where c_r and ϵ_r represent the balancing coefficients and total DFT energies per formula unit, respectively. In Table S1 in the Supplemental Material we list all unaries, binaries, and ternaries available for the Ti-Al-C system and a few possible combinations of reference phases, including balancing coefficients as an example [29]. In Table S2, we present a complete list of competing phases that are considered in the thermodynamic stability evaluation, along with the most competing phases for each MAX phase that has $\Delta_r H \leqslant +150$ meV/atom [29].

B. Efficient evaluation of competing phases

The evaluation of the maximum formation energy $\Delta_r H$ [Eq. (1)] requires the calculation of total energies for a huge number of possible competing phases (about 10 000 in total). These calculations are circumvented by the following two-step procedure. In the first step, we crudely approximate the total energy of a phase in GPAW by exploiting available data from MP [28] and OQMD [22]. An estimate of the total energy of a competing phase is obtained by summing up the reported formation enthalpy $\Delta_f H^{\mathrm{db}}$ from the databases and our calculated total energies of elemental reference phases ϵ_{el},

$$\epsilon_r^{\mathrm{est}} = \Delta_f H^{\mathrm{db}} + \sum_{\mathrm{elements}} c_{\mathrm{el}} \epsilon_{\mathrm{el}}, \quad (2)$$

where c_{el} represents the proportions per formula of an elemental constituent. The estimates are used to compute the maximum formation energy of each MAX phase. In the second step, we explicitly compute the total energies of those boundary phases of every MAX phase for which $\Delta_r H < +150$ meV/atom. With this filter, the number of explicit DFT calculations for boundary phases reduces to about only 160. Eventually, $\Delta_r H$ is reevaluated using the explicitly computed total energies of these boundary phases.

C. Computational details

High-throughput DFT calculations are performed in a spin-polarized electronic state within the framework of the projector augmented wave [30] using the open-source DFT code GPAW [31,32] in conjunction with the atomic simulation environment [33]. Electronic exchange-correlation (XC) interactions are provided by the generalized gradient approximation (GGA) in the parametrization of Perdew, Burke, and Ernzerhof (PBE) [34]. To converge formation enthalpies, an energy cutoff of 1200 eV for the plane-wave expansion of the wave functions along with k meshes with a density of 4 Å is used for MAX phases. The structural relaxation including the positions and cell was done until forces and stresses converged within 0.01 eV Å^{-1} and 0.01 eV Å^{-3}, respectively. For electronic self-consistency iterations, the default criteria of GPAW are used for convergence. Convergence studies have been performed separately for a few MAX phases to ensure the variance of total energy within an error bar of 0.1 meV/atom (see the Supplemental Material [29], Fig. S1). For each individual unary and a selection of competing phases, the convergence of the k mesh was also done until energy differences were within 0.5 meV/atom.

To include the contribution of magnetism in the formation enthalpies and to determine the magnetic properties of MAX phases, spin-polarized DFT calculations were initially performed for all 1200 MAX compositions in the ferromagnetic (FM) state. The phases that preserved net magnetization during structural optimization were later on subjected to a magnetic ground state search by calculating the total DFT energies of all possible symmetrically unique magnetic spin configurations in FM and antiferromagnetic (AFM) orderings within a conventional unit cell. Figure 2 presents all symmetrically nonequivalent magnetic configurations that are possible in a conventional unit cell of M_2AX and M_3AX_2 (MAX) phases (for M_4AX_3, see the Supplemental Material [29], Fig. S7). Naturally, the lowest energy configuration is selected for the final analysis of formation enthalpy and represents the predicted ground state ordering at 0 K. As for the competing phases, spin-polarized DFT calculations are performed only if a phase possesses nonzero magnetic moments according to the data present in online DFT databases (i.e., MP or OQMD). At the beginning of the electronic self-consistency cycle, the magnetic moments are initialized at the highest possible oxidation state of elements and are allowed to vary during the cycle. Only GGA without U approximation is employed for all calculations because identifying appropriate U values for each MAX phase and competing phase is out of the scope of the current study.

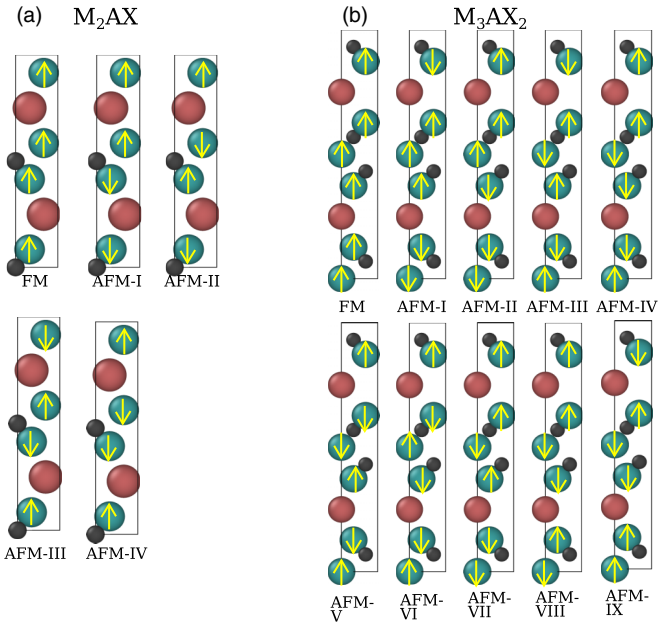

FIG. 2. All symmetrically unique spin configurations of (a) M_2AX- and (b) M_3AX_2-type MAX phases considered that are possible within a primitive cell. The unique configurations of a M_4AX_3-type MAX phase are provided in Fig. S7 in the Supplemental Material [29].

III. RESULTS AND DISCUSSION

A. Stability criterion

We first determine a threshold value for calculated formation enthalpies, below which a MAX phase may be considered metastable. Figure 3 shows calculated values of $\Delta_r H$ for a number of MAX phases. MAX phases that have been reported in the literature are separated by a dashed horizontal line from MAX phases for which only unsuccessful attempts are known to date (unfortunately, unsuccessful attempts are typically not reported in the literature, so we here rely on private communication with colleagues working experimentally [38]). Most of the stable MAX phases show a negative value of $\Delta_r H$. The maximum (positive) calculated value is 18 meV/atom (for Zr_2AlC). Concerning unstable (not synthesized) MAX phases, our data are fairly limited. While Nb_2AlN shows a maximum formation enthalpy as large as 100 meV/atom, a value as low as 4 meV/atom is found for Hf_2AlN. Thus, a sharp boundary between unstable and (meta)stable is not defined. Using the maximum calculated value of +20 meV/atom (rounded from +18 meV/atom) and allowing for 10 meV/atom error due to the PBE XC functional and pseudopotentials (see the Supplemental Material [29], Fig. S8), we determined that calculated formation enthalpies of up to +30 meV/atom may indicate potential (meta)stability and will consider that a threshold. To be more specific, we divide stability into three categories: (I) most likely stable if $\Delta_r H < -10$ meV/atom, (II) most likely

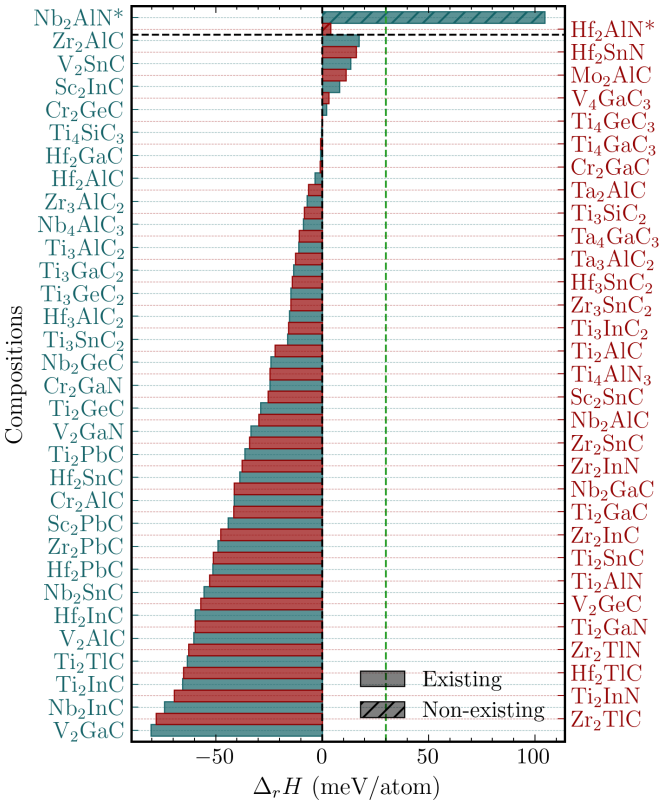

FIG. 3. Validation of the maximum formation enthalpy $\Delta_r H$ as a descriptor for thermodynamic stability. For 65 experimentally reported MAX phases, only 7 MAX phases show a positive value of $\Delta_r H$. Thermodynamic (meta)stability is indicated by $\Delta_r H < +30$ meV/atom (marked by the vertical dotted line). The compositions in the bottom part are known to synthesize (taken from Refs. [27,35–37]), while the two at the top could not be synthesized despite several experimental attempts [38].

unstable if $\Delta_r H > +30$ meV/atom, and (III) potentially stable or metastable if $-10 < \Delta_r H < +30$ meV/atom.

B. MAX phase stability

Figure 4 lists all MAX carbides (top panels) and nitrides (bottom panels) that belong to either category I (CI; $\Delta_r H < -10$, dark red background color) or category III (CIII; $\Delta_r H < +30$, light red or green background color). The full data set of all considered MAX phases is given in Sec. S2 of the Supplemental Material [29]. MAX phases that have been experimentally verified are highlighted by a solid green frame; MAX phases that have been predicted on the basis of previous calculations but for which no successful synthesis has been reported are highlighted by black frames.

We find that out of all 1200 possible MAX phases considered here, only 77 are predicted to be stable ($\Delta_r H < -10$ meV/atom) within CI, and 137 may be considered metastable or, at best, potentially stable ($-10 < \Delta_r H < +30$ meV/atom) in CIII. Out of these, 65 have been reported experimentally. Moreover, 25 MAX phases have been predicted by others but have not been synthesized yet. The rest of the phases, 986 in total, are predicted to be unstable ($\Delta_r H > +30$ meV/atom), making up category II (CII). In total, our calculations add 124 (CI and CIII) new potential MAX phases. Out of these, 7 (0 CI, 7 CIII) are M_2AC, 22 (10 CI, 12 CIII) are M_3AC_2, and 25 (4 CI, 21 CIII) are M_4AC_3; 9 (1 CI, 8 CIII) are M_2AN, 30 (2 CI, 28 CIII) are M_3AN_2, and 31 (9 CI, 22 CIII) are M_4AN_3.

C. Origin of (in)stability with increasing MX layers

The influence of the number of MX layers on the stability can be easily studied with the formation enthalpy ΔE_f (not to be confused with the maximum formation enthalpy $\Delta_r H$) calculated against unary constituents,

$$\Delta E_f = \frac{\epsilon_{\mathrm{MAX}} - \sum_i c_i \epsilon_i}{N_{\mathrm{atoms}}}, \tag{3}$$

where c is a stoichiometric amount of a constituent element i in a given MAX phase. Figure 5(a) shows the dependence of the formation enthalpy (with respect to the constituents) on the number of layers n in Al-based MAX carbides. Like for $\Delta_r H$ (see the Supplemental Material [29], Fig. S6), two distinctive trends are found but are more clearly distinguishable: (1) a slight or no decrease in ΔE_f with n in early transition metals (Sc, Ti, V; blue points) indicates an increase in stability with the addition of an MX layer, and (2) on the contrary, late transition metals (Cr and onwards; green points) have an increase in ΔE_f with increasing n, pointing towards a reduction in the stability with the addition of an MX layer. To understand the origin of these distinctive trends in the formation enthalpy, formation enthalpies with respect to constituents of A- and X-centered trigonal prism and octahedral configurations of M, respectively, are evaluated. These configurations are the building blocks of a MAX crystal structure [see the inset in Fig. 5(b)]. Figure 5(b) shows calculated formation enthalpies of $3d$ transition metals with Al and C. In early transition metals (Sc, Ti, V; blue bars), ΔE_f of an MX_6 octahedron is significantly lower than that of an MA_6 trigonal prism, indicating a gain in energy from adding more MX layers. However, this energy gain is partially compensated due to distortion of the MX_6 octahedron [40] when placed together inside a MAX structure. So the overall effect would show up only as a slight or no decrease in the formation enthalpy (and, consequently, stability) of the corresponding MAX phases when increasing the number of MX layers. Conversely, late transition metals (Cr and onwards; green bars) form energetically unfavored MX_6 octahedrons compared to trigonal prisms. This means there is no gain in energy by adding further MX layers. Additionally, the energy contribution due to octahedral distortion is also positive. This results in a rise not only in formation enthalpy but also in positive values (unstable).

The origin of the difference in formation enthalpies of early and late transition metals with carbon is the availability of valence electrons, which is known in the literature for binary transition metal carbides [41,42]. If a sufficient number of valence electrons are available to fill the bonding hybridized states of M(dp)-C(sp), the formation energy decreases due to stronger bonding and is observed in early transition metals. On the contrary, late transition metals have an abundance of valence electrons that also occupy antibonding hybridized states and bond weakly with C. This is also backed by the

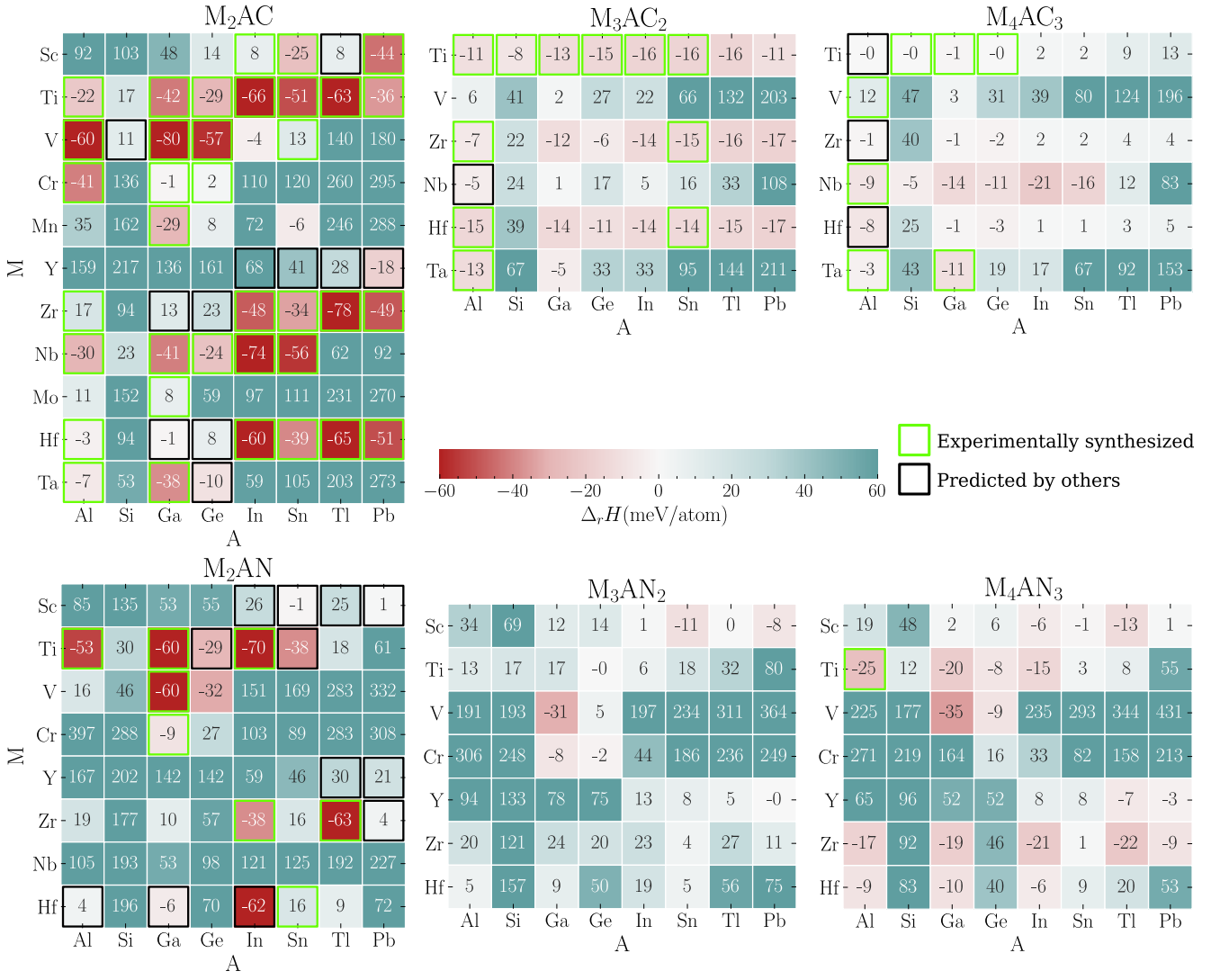

FIG. 4. Maximum formation enthalpies $\Delta_r H$ for various MAX carbides and nitrides of type $n = 1, 2, 3$ composed of different M and A elements; $\Delta_r H < +30$ meV/atom indicates potential (meta)stability. The red (turquoise) shaded background of individual entries indicates a negative (positive) maximum formation enthalpy; the intensity increases with increasing (absolute) magnitude. MAX phases that have been reported experimentally [27,35–37] and theoretically by others [26,39] are further highlighted by green and black frames, respectively. We note that only the M and A elements for which stable combinations exist are listed here; the full list of all considered MAX phases is provided in Sec. S2. of the Supplemental Material [29].

fact that late transition metals do not form stable binary MC rocksalt crystal phases [43].

Based on the relative difference in the formation enthalpies of MX_6 and MA_6 building blocks, some crucial observations related to thermodynamic stability can be deduced. If M_2AC is stable, then higher n MAX phases will also be stable on the condition that ΔE_f of the MX_6 octahedron is lower than that of the MA_6 trigonal prism. For example, all MAX compositions in Ti-Al-C and V-Al-C are (meta) stable.

D. Stability descriptors

As mentioned above, an excess of valence electrons seems to cause a reduction in the stability. In this respect, VEC, as defined by Eq. (4), has been demonstrated in the literature to have a correlation with the stability of MAX phases [20,44], thus making it one of the necessary criteria for stability:

$$\mathrm{VEC} = \frac{\sum_{M,A,X} m_i v_i}{N_{\mathrm{total}}}. \tag{4}$$

Here, m is the number of M, A, and X atoms in a formula unit, and v is the number of valence electrons of a particular element. The transition metals are treated to contain noble gas + n valence electrons (e.g., Sc has Ar + 3 valence electrons); for the nonmetallic elements, including C and N, the group number determines the number of valence electrons. N_{total} is the total number of atoms per formula unit. Here, we try to investigate and validate a correlation between VEC and the stability of ternary MAX carbides and nitrides. Figure 6 shows the relationship between VEC and $\Delta_r H$ for all MAX compositions studied here. It is observed that a specific region in VEC is preferred by the MAX phases that are stable or

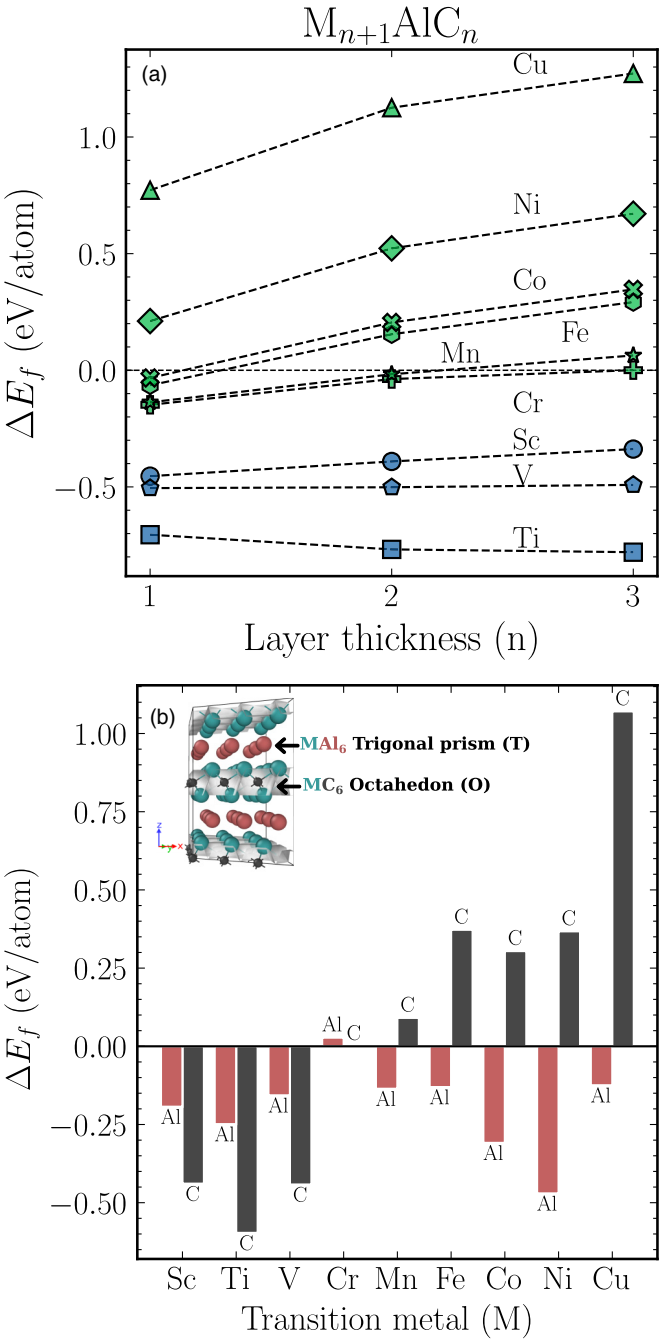

FIG. 5. (a) The effect of varying the number of MX layers as defined by n on formation enthalpy with respect to unary constituents (ΔE_f) of Al-containing MAX carbides of 3d transition metals. Two different behaviors are visible: (1) an increase in ΔE_f for late transition metals, e.g., Cr, Fe, etc., and (2) a decrease or negligible change in ΔE_f with n. The color coding marks the respective trend. (b) Calculated formation enthalpies with respect to unary constituents of the C- and Al-centered octahedron (O) and trigonal prism (T), respectively, which are the building blocks of a MAX phase (see the inset).

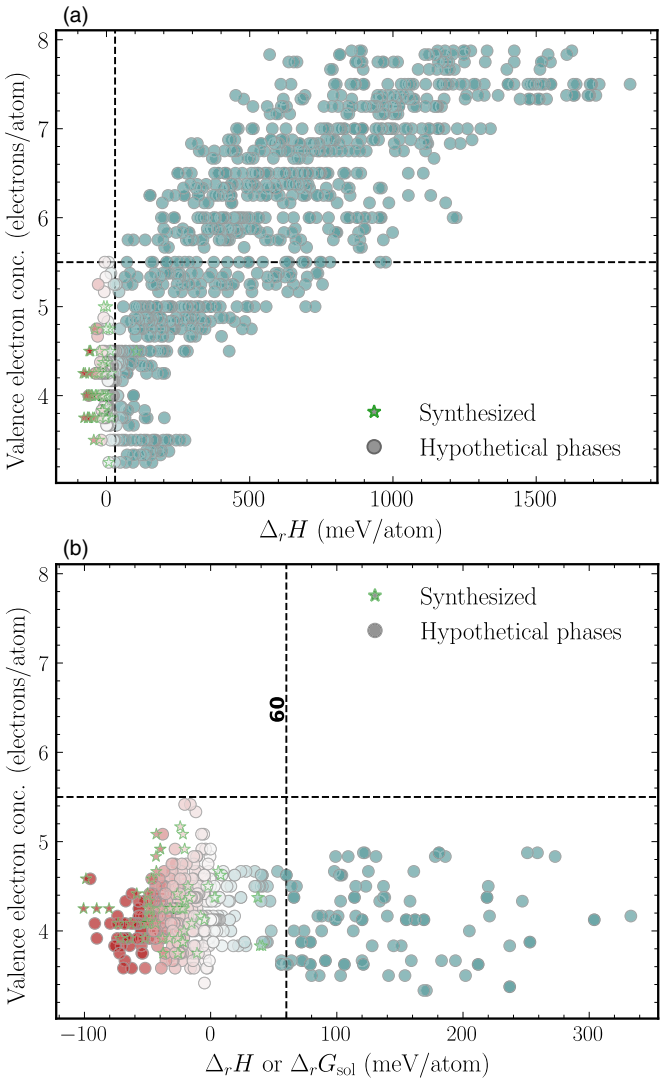

FIG. 6. (a) Correlation of the valence electron concentration (VEC) per atom with the maximum formation enthalpy $\Delta_r H$ of all 1200 compositions studied in this work. (b) Usage and validation of VEC as a potential instability descriptor for identifying unstable ordered and disordered double MM′AX phases that have been studied by others [19,26]. In (b) $\Delta_r H$ (at 0 K) and $\Delta_r G_{sol}$ (at 2000 K) are plotted for ordered and disordered phases, respectively. $\Delta_r G_{sol}$ is the free energy of a disordered phase (solid solution) at a particular temperature (solid solution) and is defined in detail in Ref. [19]. The vertical line marks the (meta)stability limit at (a) 30 meV/atom and (b) 60 meV/atom as used in Ref. [19] for (dis)ordered phases. All the unstable phases in (a) have VEC above ∼5.5 electrons/atom (horizontal dashed line), which is verified by (b), demonstrating VEC as a general thermodynamic instability descriptor. The color gradient of the scatter is the same as in Fig. 4.

metastable (CI and CIII); that is, all the stable or metastable phases lie below 5.5 VEC. Above this limit, the phases are unstable, as indicated by large positive values of $\Delta_r H$. This instability is known to be caused by the gradual filling of the antibonding states in a MAX phase, a well-known phenomenon for binary carbides and nitrides [42] that has also been investigated fairly well for ternary MAX phases [45]. However, we emphasize that VEC < 5.5 is only a necessary criterion, not a sufficient one; many entries are present for VEC < 5.5 that have positive and high ($> +30$ meV/atom) $\Delta_r H$, indicative of their instability. The VEC does not seem to have a direct correlation with $\Delta_r H$ and thus cannot fully

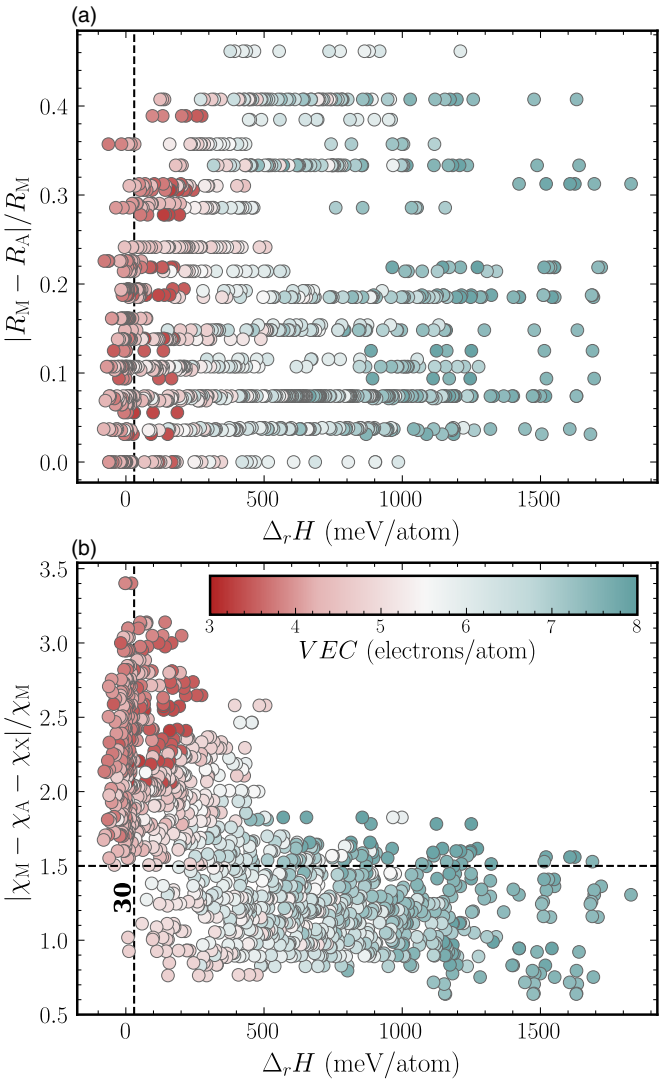

FIG. 7. Relationship of (a) radius differences ΔR_{at} and (b) electronegativity differences $\Delta\chi$ of M, A, and X atoms, with maximum formation enthalpy $\Delta_r H$ and VEC. ΔR_{at} values are scattered throughout the $\Delta_r H$ range. Below $\Delta\chi$ of ~1.5 (horizontal dashed line), the majority of the phases are unstable; an indirect correlation with $\Delta_r H$ and VEC exists. The vertical line marks the (meta)stability limit at +30 meV/atom. The electronegativities and atomic radii are taken from data available in PYMATGEN [46].

describe the stability. However, based on Fig. 6, the VEC can give an initial indication of the potential (meta)stability of a MAX phase and can thus partially describe stability.

To fully describe the stability, descriptors in addition to VEC are necessary. One such descriptor discussed in the literature [44] is the atomic radius differences of M and A. We have screened atomic radius differences ΔR_{at} and, additionally, electronegativity differences $\Delta\chi$ as potential descriptors, as shown in Figs. 7(a) and 7(b), respectively. Out of these two, only $\Delta\chi$ indirectly correlates with $\Delta_r H$; that is, all stable or metastable phases (except two) have $\Delta\chi$ above 1.5. Similar to VEC, this criterion is also not sufficient to fully describe the stability as many unstable entries are present in the $\Delta\chi > 1.5$ region. Therefore, combining both descriptors moderately improves the predictive power. Unfortunately, $\Delta\chi$ is also strongly correlated with VEC [Fig. 7(b)], and it is not possible to directly apply $\Delta\chi$ for predicting double MM′AX phases because of an additional parameter $\chi_{M'}$ in this case. It is ambiguous whether similar values of χ for M and M′ or their average or weighted average above an unknown threshold matters for stability.

Nevertheless, based on Fig. 6, VEC can be used as an instability descriptor to rule out a big chunk of unstable MAX phases. A favorable region in VEC suggests that a low-valence metal can be doped with a high-valence metal to incorporate the latter into the MAX structure to fine-tune properties of interest.

Figure 6(b) shows VEC as a potential descriptor of instability for double MM′AX phases. Double MM′AX phases have two transitional metals at the M site, distributed randomly or in a certain order. Due to configurational degrees of freedom, using DFT calculations to predict stable phases requires immense effort. Having a descriptor that can correlate with $\Delta_r H$ for such phases is significant. Here, in an attempt to find such a descriptor, we validate and test VEC for predicted or already synthesized double MM′AX phases to date that are found in the literature [19,26]. Figure 6(b) contains VEC vs the maximum formation enthalpy $\Delta_r H$ of ordered phases and maximum free energy $\Delta_r G_{sol}$ (which includes entropic contributions, defined in [19]) of disordered double MM′AX phases of type $(M, M')_{n+1}AC_n (n = 1, 2, 3)$. (The data for the plots were obtained from Refs. [19,26]. Moreover, compositions that are unconventional, i.e., have the transition metal at the A site, are excluded in the current analysis.) VEC is found to be below 5.5 for all predicted or existing MM′AX phases, verifying VEC is a potential instability descriptor. Therefore, VEC can be used to prescreen a huge chemical space of double-M-containing MM′AX to narrow down the search for potential phases more efficiently without performing any DFT calculations.

E. Magnetic MAX phases

Figure 8 shows the magnetic moment of MAX phases that are found to be magnetic in either the FM or AFM state. Out of 214 (meta)stable MAX phases (CI and CIII), 9 phases are predicted to be magnetic, 4 of which have already been experimentally synthesized [47–50]. Cr_2AlC and Mn_2GaC (which exist only as a thin film) have FM ordering; the former is a weak FM with $0.01\mu_B$/Cr, that agrees fairly well with experiments [47,51], while the latter has a high magnetic moment of $1.88\mu_B$/Mn. However, Mn_2GaC was found experimentally to have noncollinear AFM ordering [52] and theoretically to have a $2.0\mu_B$/Mn magnetic moment [53]. This discrepancy between our result and experiment is caused by not considering noncollinear AFM configurations in our magnetic ground state search procedure. The energy difference between the FM and noncollinear AFM configurations is reported to be as little as 1 meV/atom [53].

The rest of the phases are antiferromagnetically ordered with a zero net magnetization, except for Cr_3GaN_2 and Cr_4GeN_3, which have unequal opposing magnetic moments along the z axis, so that a net magnetization remains, marking them as ferrimagnetic (FiM). Here, we predict, for the first

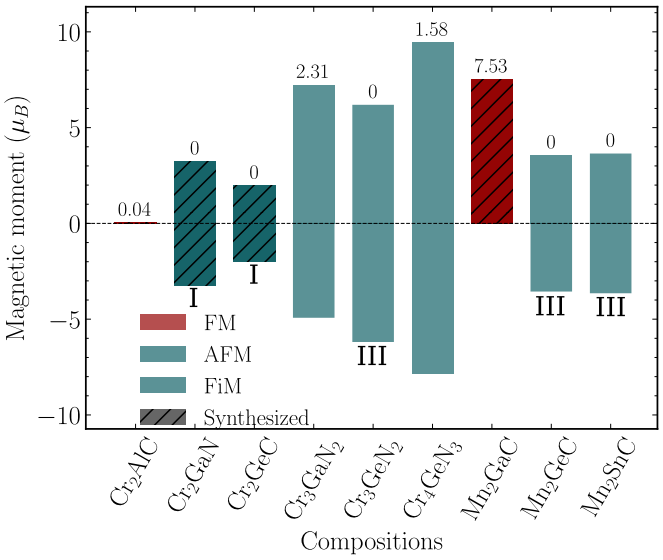

FIG. 8. Calculated magnetic moments of numerous MAX phases that are found to be magnetic, out of 1200 compositions studied here. The experimentally synthesized compositions are denoted by a check pattern. FM, AFM, and FiM represent ferromagnetic, antiferromagnetic, and ferrimagnetic order, respectively. The label at the top of each bar is the total magnetization. All the symmetrically unique spin configurations of a M_2AX-and M_3AX_2-type MAX phase are shown in Fig. 2, whereas that of a M_4AX_3-type MAX phase are provided in Fig. S7 in the Supplemental Material [29].

time, two ferrimagnetic MAX phases. The magnetic ground spin configuration of the AFM MAX phases is also indicated in Fig. 8, and all possible magnetic spin configurations are shown in Fig. 2 and in Fig. S7 of the Supplemental Material [29]. Cr_2GaN and Cr_2GeC have an AFM-I magnetic ground state, while Mn_2(A=Ge,Sn)C and Cr_3GeN_2 have an AFM-III magnetic ground state.

In total, we found five new magnetic MAX phases (three are AFM and two are FiM) that are potentially (meta)stable, including a M_4AX_3 type of MAX phase.

IV. CONCLUSION

In this work, we have carried out high-throughput DFT calculations to screen about 1200 MAX compositions for potential (meta)stability. Out of these compositions, 124 new phases are predicted to be (meta)stable in the sense of having negative or only slightly positive maximum formation enthalpies relative to boundary phases. Out of these phases, 54 and 70 are carbides and nitrides, respectively. Only five of the predicted phases are found to have long-range magnetic order and contain Cr and Mn as M transition metals. Among the previously suggested descriptors of stability, we found that only VEC and $\Delta\chi$ correlate with stability. It was found that a region in VEC and $\Delta\chi$ that lies below ∼5.5 and above ∼1.5 is preferred by all stable and synthesized MAX phases. Any phase that is found outside of these limits is unstable, as indicated by the positive and high magnitude of $\Delta_f H$. However, the reverse is not true. VEC has been successfully validated for all double MM′AX phases that are known or predicted to date, suggesting it is useful for providing an initial firsthand guess about the stability of a MAX phase without doing any theoretical or experimental work. Furthermore, based on the VEC, it was suggested that the inclusion of late transition metals (e.g., Fe, Ni, Co, etc.) can be made possible by doping the M site with a low-valence transition metal (e.g., Sc, V, Ti). Using $\Delta\chi$ for double MM′AX is ambiguous due to the introduction of an additional parameter, $\chi_{M'}$.

ACKNOWLEDGMENTS

This research is financially supported by the German Research Foundation (DFG) within "CRC/TRR 270 Hysteresis design of magnetic materials for efficient energy conversion: HoMMage" (Project No. 405553726) via project B07 and by a DFG grant, "Theory guided synthesis of MXenes with magnetic ordering" (Project No. 501386284). The authors gratefully acknowledge the computing time provided to them on the high-performance computer Lichtenberg at the NHR Centers NHR4CES at TU Darmstadt. It is funded by the Federal Ministry of Education and Research and the state governments participating on the basis of the resolutions of the GWK for national high-performance computing at universities. The authors also are grateful to Dr. C. Birkel and N. Kubitza for insightful discussions and for providing experimental data.

[1] M. W. Barsoum and T. El-Raghy, Synthesis and characterization of a remarkable ceramic: Ti_3SiC_2, J. Am. Ceram. Soc. **79**, 1953 (1996).

[2] J. W. Byeon, J. Liu, M. Hopkins, W. Fischer, N. Garimella, K. B. Park, M. P. Brady, M. Radovic, T. El-Raghy, and Y. H. Sohn, Microstructure and residual stress of alumina scale formed on Ti_2AlC at high temperature in air, Oxid. Met. **68**, 97 (2007).

[3] M. W. Barsoum and M. Radovic, Elastic and mechanical properties of the MAX phases, Annu. Rev. Mater. Res. **41**, 195 (2011).

[4] M. Haftani, M. S. Heydari, H. R. Baharvandi, and N. Ehsani, Studying the oxidation of Ti_2AlC MAX phase in atmosphere: A review, International J. Refractory Metals Hard Mater. **61**, 51 (2016).

[5] R. Grieseler, M. K. Camargo, M. Hopfeld, U. Schmidt, A. Bund, and P. Schaaf, Copper-MAX-phase composite coatings obtained by electro-co-deposition: A promising material for electrical contacts, Surf. Coat. Technol. **321**, 219 (2017).

[6] Z. M. Sun, Progress in research and development on MAX phases: a family of layered ternary compounds, Int. Mater. Rev. **56**, 143 (2011).

[7] M. Naguib, M. Kurtoglu, V. Presser, J. Lu, J. Niu, M. Heon, L. Hultman, Y. Gogotsi, and M. W. Barsoum, Two-dimensional nanocrystals produced by exfoliation of Ti_3AlC_2, Adv. Mater. **23**, 4248 (2011).

[8] M. H. Tran, T. Schäfer, A. Shahraei, M. Dürrschnabel, L. Molina-Luna, U. I. Kramm, and C. S. Birkel, Adding a new member to the MXene family: Synthesis, structure, and electrocatalytic activity for the hydrogen evolution reaction of $V_4C_3T_x$, ACS Appl. Energy Mater. **1**, 3908 (2018).

[9] Y. Gogotsi and B. Anasori, The rise of MXenes, ACS Nano **13**, 8491 (2019).

[10] M. Dahlqvist, B. Alling, and J. Rosén, Stability trends of MAX phases from first principles, Phys. Rev. B **81**, 220102(R) (2010).

[11] S. Aryal, R. Sakidja, M. W. Barsoum, and W. Y. Ching, A genomic approach to the stability, elastic, and electronic properties of the MAX phases, Phys. Status Solidi B **251**, 1480 (2014).

[12] M. Ashton, R. G. Hennig, S. R. Broderick, K. Rajan, and S. B. Sinnott, Computational discovery of stable M_2AX phases, Phys. Rev. B **94**, 054116 (2016).

[13] C. M. Hamm, T. Schäfer, H. Zhang, and C. S. Birkel, Nonconventional synthesis of the 413 MAX phase V_4AlC_3, Z. Anorg. Allg. Chem. **642**, 1397 (2016).

[14] Q. Tao, T. Ouisse, D. Pinek, O. Chaix-Pluchery, F. Wilhelm, A. Rogalev, C. Opagiste, L. Jouffret, A. Champagne, J.-C. Charlier, J. Lu, L. Hultman, M. W. Barsoum, and J. Rosen, Rare-earth (RE) nanolaminates $Mo_4RE_4Al_7C_3$ featuring ferromagnetism and mixed-valence states, Phys. Rev. Mater. **2**, 114401 (2018).

[15] N. C. Frey, J. Wang, G. I. V. Bellido, B. Anasori, Y. Gogotsi, and V. B. Shenoy, Prediction of synthesis of 2D metal carbides and nitrides (MXenes) and their precursors with positive and unlabeled machine learning, ACS Nano **13**, 3031 (2019).

[16] Q. Tao *et al.*, Atomically layered and ordered rare-earth i-MAX phases: A new class of magnetic quaternary compounds, Chem. Mater. **31**, 2476 (2019).

[17] N. Miao, J. Wang, Y. Gong, J. Wu, H. Niu, S. Wang, K. Li, A. R. Oganov, T. Tada, and H. Hosono, Computational prediction of boron-based MAX phases and MXene derivatives, Chem. Mater. **32**, 6947 (2020).

[18] N. Kubitza, A. Reitz, A. M. Zieschang, H. Pazniak, B. Albert, C. Kalha, C. Schlueter, A. Regoutz, U. Wiedwald, and C. S. Birkel, From MAX phase carbides to nitrides: Synthesis of V_2GaC, V_2GaN, and the carbonitride $V_2GaC_{1-x}N_x$, Inorg. Chem. **61**, 10634 (2022).

[19] M. Dahlqvist and J. Rosen, The rise of MAX phase alloys–Large-scale theoretical screening for the prediction of chemical order and disorder, Nanoscale **14**, 10958 (2022).

[20] R. Khaledialidusti, M. Khazaei, S. Khazaei, and K. Ohno, High-throughput computational discovery of ternary-layered MAX phases and prediction of their exfoliation for formation of 2D MXenes, Nanoscale **13**, 7294 (2021).

[21] J. E. Saal, S. Kirklin, M. Aykol, B. Meredig, and C. Wolverton, Materials design and discovery with high-throughput density functional theory: The open quantum materials database (OQMD), JOM 2013 65:11 **65**, 1501 (2013).

[22] S. Kirklin, J. E. Saal, B. Meredig, A. Thompson, J. W. Doak, M. Aykol, S. Rühl, and C. Wolverton, The Open Quantum Materials Database (OQMD): Assessing the accuracy of DFT formation energies, npj Comput. Mater. **1**, 15010 (2015).

[23] A. Mockute, M. Dahlqvist, J. Emmerlich, L. Hultman, J. M. Schneider, P. O. A. Persson, and J. Rosen, Synthesis and *ab initio* calculations of nanolaminated $(Cr,Mn)_2AlC$ compounds, Phys. Rev. B **87**, 094113 (2013).

[24] M. Dahlqvist, B. Alling, I. A. Abrikosov, and J. Rosen, Magnetic nanoscale laminates with tunable exchange coupling from first principles, Phys. Rev. B **84**, 220403 (2011).

[25] M. Dahlqvist, J. Lu, R. Meshkian, Q. Tao, L. Hultman, and J. Rosen, Prediction and synthesis of a family of atomic laminate phases with kagomé-like and in-plane chemical ordering, Sci. Adv. **3**, e1700642 (2017).

[26] M. Dahlqvist and J. Rosen, Predictive theoretical screening of phase stability for chemical order and disorder in quaternary 312 and 413 MAX phases, Nanoscale **12**, 785 (2020).

[27] M. Sokol, V. Natu, S. Kota, and M. W. Barsoum, On the chemical diversity of the MAX phases, Trends Chem. **1**, 210 (2019).

[28] A. Jain, S. P. Ong, G. Hautier, W. Chen, W. D. Richards, S. Dacek, S. Cholia, D. Gunter, D. Skinner, G. Ceder, and K. A. Persson, Commentary: The materials project: A materials genome approach to accelerating materials innovation, APL Mater. **1**, 011002 (2013).

[29] See Supplemental Material at http://link.aps.org/supplemental/10.1103/PhysRevMaterials.7.044408 for technical details, the set of competing phases, and the formation enthalpies of the complete list of studied MAX phases.

[30] P. E. Blöchl, Projector augmented-wave method, Phys. Rev. B **50**, 17953 (1994).

[31] J. J. Mortensen, L. B. Hansen, and K. W. Jacobsen, Real-space grid implementation of the projector augmented wave method, Phys. Rev. B **71**, 035109 (2005).

[32] J. Enkovaara *et al.*, Electronic structure calculations with GPAW: A real-space implementation of the projector augmented-wave method, J. Phys.: Condens. Matter **22**, 253202 (2010).

[33] A. H. Larsen *et al.*, The atomic simulation environment—A python library for working with atoms, J. Phys.: Condens. Matter **29**, 273002 (2017).

[34] J. P. Perdew, K. Burke, and M. Ernzerhof, Generalized Gradient Approximation Made Simple, Phys. Rev. Lett. **77**, 3865 (1996).

[35] Q. Xu, Y. Zhou, H. Zhang, A. Jiang, Q. Tao, J. Lu, J. Rosén, Y. Niu, S. Grasso, and C. Hu, Theoretical prediction, synthesis, and crystal structure determination of new MAX phase compound V_2SnC, J. Adv. Ceram. **9**, 481 (2020).

[36] Y. Li, Y. Qin, K. Chen, L. Chen, X. Zhang, H. Ding, M. Li, Y. Zhang, S. Du, and Z. Chai, Molten salt synthesis of nanolaminated Sc_2SnC MAX phase, J. Inorg. Mater. **36**, 773 (2021).

[37] Q. Zhang, B. Wen, J. Luo, Y. Zhou, X. San, Y. Bao, Q. Feng, S. Grasso, and C. Hu, Synthesis of new rare earth containing ternary laminar Sc_2PbC ceramic, J. Eur. Ceram. Soc. **43**, 1735 (2023).

[38] N. Kubitza, Unsuccessful synthesis attempts of Nb_2AlN and Hf_2AlN (unpublished).

[39] D. Ohmer, G. Qiang, I. Opahle, H. K. Singh, and H. Zhang, High-throughput design of 211-M_2AX compounds, Phys. Rev. Mater. **3**, 053803 (2019).

[40] G. Hug, M. Jaouen, and M. W. Barsoum, X-ray absorption spectroscopy, EELS, and full-potential augmented plane wave study of the electronic structure of Ti_2AlC, Ti_2AlN, Nb_2AlC, and $(Ti_{0.5}Nb_{0.5})_2AlC$, Phys. Rev. B **71**, 024105 (2005).

[41] C. D. Gelatt, A. R. Williams, and V. L. Moruzzi, Theory of bonding of transition metals to nontransition metals, Phys. Rev. B **27**, 2005 (1983).

[42] J. Häglund, A. Fernández Guillermet, G. Grimvall, and M. Körling, Theory of bonding in transition-metal carbides and nitrides, Phys. Rev. B **48**, 11685 (1993).

[43] I. Khatri, N. J. Szymanski, B. B. Dumre, J. G. Amar, D. Gall, and S. V. Khare, Correlating structure and orbital occupation with the stability and mechanical properties of 3d transition metal carbides, J. Alloys Compd. **891**, 161866 (2022).

[44] Y. Zhang, Z. Mao, Q. Han, Y. Li, M. Li, S. Du, Z. Chai, and Q. Huang, The role of Hume-Rothery's rules play in the MAX phases formability, Materialia **12**, 100810 (2020).

[45] M. Khazaei, M. Arai, T. Sasaki, M. Estili, and Y. Sakka, Trends in electronic structures and structural properties of MAX phases: A first-principles study on M_2AlC (M = Sc, Ti, Cr, Zr, Nb, Mo, Hf, or Ta), M_2AlN, and hypothetical M_2AlB phases, J. Phys.: Condens. Matter **26**, 505503 (2014).

[46] S. P. Ong, W. D. Richards, A. Jain, G. Hautier, M. Kocher, S. Cholia, D. Gunter, V. L. Chevrier, K. A. Persson, and G. Ceder, Python materials genomics (pymatgen): A robust, open-source python library for materials analysis, Comput. Mater. Sci. **68**, 314 (2013).

[47] M. Jaouen, P. Chartier, T. Cabioc'h, V. Mauchamp, G. André, and M. Viret, Invar like behavior of the Cr_2AlC MAX phase at low temperature, J. Am. Ceram. Soc. **96**, 3872 (2013).

[48] Z. Liu, T. Waki, Y. Tabata, K. Yuge, H. Nakamura, and I. Watanabe, Magnetic ground state of the $M_{n+1}AX_n$-phase nitride Cr_2GaN, Phys. Rev. B **88**, 134401 (2013).

[49] Z. Liu, T. Waki, Y. Tabata, and H. Nakamura, Mn-doping-induced itinerant-electron ferromagnetism in Cr_2GeC, Phys. Rev. B **89**, 054435 (2014).

[50] A. S. Ingason, A. Petruhins, M. Dahlqvist, F. Magnus, A. Mockute, B. Alling, L. Hultman, I. A. Abrikosov, P. O. Persson, and J. Rosen, A nanolaminated magnetic phase: Mn_2GaC, Mater. Res. Lett. **2**, 89 (2014).

[51] M. Jaouen, M. Bugnet, N. Jaouen, P. Ohresser, V. Mauchamp, T. Cabioc'h, and A. Rogalev, Experimental evidence of Cr magnetic moments at low temperature in Cr_2A(A=Al, Ge)C, J. Phys.: Condens. Matter **26**, 176002 (2014).

[52] I. P. Novoselova, A. Petruhins, U. Wiedwald, Á. Sigurdur Ingason, T. Hase, F. Magnus, V. Kapaklis, J. Palisaitis, M. Spasova, M. Farle, J. Rosen, and R. Salikhov, Large uniaxial magnetostriction with sign inversion at the first order phase transition in the nanolaminated Mn_2GaC MAX phase, Sci. Rep. **8**, 2637 (2018).

[53] A. Thore, M. Dahlqvist, B. Alling, and J. Rosén, First-principles calculations of the electronic, vibrational, and elastic properties of the magnetic laminate Mn_2GaC, J. Appl. Phys. **116**, 103511 (2014).